

Equilibrium, Kinetics, and Thermodynamic Evaluation of Mercury (II) Removal from Aqueous Solutions by Moss (*Homalothecium sericeum*) Biomass

Duygu Ozdes^a and Celal Duran^b

^aGumushane Vocational School, Gumushane University, Gumushane 29100, Turkey

^bDepartment of Chemistry, Faculty of Sciences, Karadeniz Technical University, Trabzon 61080, Turkey; cduran@ktu.edu.tr (for correspondence)

Published online 5 June 2015 in Wiley Online Library (wileyonlinelibrary.com). DOI 10.1002/ep.12166

In the present research, *Homalothecium Sericeum* was utilized for the first time as an effective and readily available adsorbent in removal of Hg(II) ions from aqueous solutions through a batch adsorption technique. The effects of initial solution pH, contact time, initial Hg(II) and adsorbent concentration, temperature, and ionic strengths were evaluated on the removal efficiency of Hg(II) ions, after being characterized of *H. sericeum* by different techniques. The maximum Hg(II) adsorption was obtained as 128.2 mg g⁻¹ at initial pH 6.0 with an equilibrium time of 60 min, adsorbent dosage of 5.0 g L⁻¹ and initial Hg(II) concentration range of 50–750 mg L⁻¹. The adsorption behaviors of Hg(II) ions onto *H. sericeum* were investigated in terms of kinetics (pseudo-first order, pseudo-second order, and intraparticle diffusion models), isotherms (Langmuir, Freundlich, and Dubinin Radushkevich models), and thermodynamics evaluation. Both the Langmuir and Freundlich isotherm models were found to be suitable to describe the adsorption equilibrium while the adsorption kinetics followed by the pseudo-second order model. Thermodynamic parameters including the Gibbs free energy (ΔG), enthalpy (ΔH), and entropy (ΔS) changes indicated that the adsorption of Hg(II) ions onto *H. sericeum* was feasible, spontaneous, and endothermic in nature. © 2015 American Institute of Chemical Engineers *Environ Prog*, 34: 1620–1628, 2015

Keywords: adsorption, *Homalothecium sericeum*, mercury (II), isotherm, kinetics

INTRODUCTION

Heavy metals, naturally occurring compounds in the earth's crust, are non-biodegradable and have high potential to accumulate in living tissues by causing several disorders and diseases even at trace levels of exposure [1]. Among the heavy metals, Hg(II), as the most toxic form of mercury, is considered as a quite hazardous element for human health [2]. Hg(II) can be readily absorbed in the gastrointestinal tract because of high solubility of its salts in water and in living

organisms, it primarily damages the gastrointestinal tract, liver, and kidney. Hg(II) also affects adversely the central nervous system by accumulating in the human brain [3,4]. Hg(II) is released to the environment through the wastes of several industrial activities including electroplating, oil refinery, pharmaceutical, paper, pulp, mining, and battery manufacturing [5,6]. According to the World Health Organization (WHO) and Environmental Protection Agency (EPA) recommendations, the maximum permissible limit for inorganic mercury in drinking water is determined as 6 and 2 $\mu\text{g L}^{-1}$, respectively [7,8]. Hence the development of cost-effective methods to remove both Hg(II) and other toxic heavy metal ions has become an important research focus.

A number of techniques such as ion exchange [9], chemical precipitation [10], membrane filtration [11], reverse osmosis [12], and adsorption [13] have been used by different researchers in treatment of water and wastewater containing toxic heavy metal ions. Among them the adsorption, by utilizing a proper adsorbent, is considered as a widely applied, practical, and effective treatment method because of its many advantages including low operating cost, short operation time, and reusability of the adsorbent. Also, the secondary compounds which may be toxic are not produced in the adsorption process [14–16]. Because the characteristics of the utilized adsorbents are directly effective on the applicability and economy of the adsorption process, the selection of the proper adsorbent is the most important issue to be considered [17]. Several adsorbents such as activated carbon produced from *Bambusa vulgaris striata* [18], chitosan-poly(vinyl alcohol) hydrogel [19], chitosan-based material [20], modified *Phoenix dactylifera* biomass [21], manganese chloride nanoparticles [22], and mosses [23] have been used for the adsorptive removal of Hg(II) ions from aqueous solutions.

Among them, mosses have high cation exchange capacity, hence most of the researchers have used them as biomonitors for the determination of heavy metal deposition for more than 20 years. In addition, they show high adsorption capacity for heavy metal ions because they have no epidermis or cuticle so heavy metal ions can easily penetrate to

their cell walls [24,25]. Based on this information, in the presented study, we have investigated the adsorption potential of a moss species, *Homalothecium sericeum*, in removal of Hg(II) ions from aqueous solutions, in order to offer an alternative to already existing adsorbents. Various moss species including *Racomitrium lanuginosum* [23], *Hylacomium splendens* [26], *Drepanocladus revolvens* [27], Romanian peat moss [28], *Poblia flexuosa* [29], and *Funaria hygrometrica* [30] have been used for the removal of Hg(II) and other toxic metal ions from aqueous solution. However, there is no reported investigation on the adsorption of Hg(II) ions by *H. sericeum*. The *H. sericeum* is one of the most abundant, effective, and cheap material since it is highly available in all over the world and has no important industrial usage. In the presented investigation, the *H. sericeum* has been utilized without any physical or chemical pretreatment, which is an important feature of the study as this reduces not only the costs but also the risks of the toxic contaminations.

First of all, we have characterized the *H. sericeum* by different techniques including FTIR, SEM, BET surface area analyses, and Boehm titration, etc. Thereafter, the effects of the experimental parameters such as initial pH of the solution, contact time, initial Hg(II) concentration, adsorbent concentration, ionic strength, and temperature were evaluated on the process in order to obtain the best adsorption conditions. The adsorption kinetics (pseudo-first-order, pseudo-second-order, and intraparticle diffusion models), isotherms (Langmuir, Freundlich, and Dubinin Radushkevich isotherm models), and thermodynamics (Gibbs free energy, enthalpy, and entropy changes) were evaluated in detail in order to reveal the adsorption mechanism.

MATERIALS AND METHODS

Adsorbent Preparation and Characterization

The moss samples (*H. sericeum*) were obtained from the East Black Sea Region of Turkey. The collected samples were washed with deionized water for several times and dried in an oven at 70°C for 48 h. The dried moss samples were ground in a blender and stored in glass containers after being sieved to particle size of <150 µm.

The specific surface area of *H. sericeum* was determined from the N₂ gas adsorption isotherm at 77 K using a TriStar 3000 (Micromeritics, USA) model specific surface area analyzer while the FTIR spectrum was recorded between 400 and 4000 cm⁻¹ in a Perkin Elmer 1600 FTIR spectrometer. SEM analysis was performed using a Zeiss Evo LS-10 type instrument. The determination of other characterization parameters of *H. sericeum* including self-pH and pH_{pzc} values, and moisture content was carried out according to standard methods [31]. Boehm titration was performed to determine the surface acidic functional groups of *H. sericeum* [32]. The characterization results are given in Table 1.

Batch Adsorption Procedure

All the chemicals used in this work were analytical grade supplied from Merck (Darmstadt, Germany) and Fluka (Buchs, Switzerland). Stock solution of 5000 mg L⁻¹ Hg(II) was prepared by dissolving appropriate amount of HgCl₂ in deionized water and the required concentration of Hg(II) solutions were prepared by dilutions of the stock solution. The adsorption tests were carried out by mixing 10–200 mg of *H. sericeum* (1.0–20.0 g L⁻¹ suspensions) with 10 mL of Hg(II) solutions in the concentration range of 50–750 mg L⁻¹ in 15 mL polyethylene centrifuge tubes. The initial pH of the Hg(II) solutions was adjusted in the range of 2.0–8.0 by the addition of dilute HNO₃ and NaOH solutions using Hanna pH-211 model digital pH meter with glass electrode. Edmund Bühler GmbH model mechanical shaker was used in the

Table 1. Characteristics of *H. sericeum*.

BET surface area (m ² g ⁻¹)	< 5
pH	6.65
pH _{pzc}	5.90
Moisture content (%)	9.28
Surface functional groups (mmol g ⁻¹)	
Carboxylic	1.38
Phenolic	4.14
Lactonic	1.38
Total acidic value	6.90

equilibrium time range of 1–240 min at 400 rpm. After sufficient equilibrium time, the suspension was centrifuged at 3000 rpm for 5 min. Hg(II) levels in the dilute phase was determined by utilizing a double beam UV-vis spectrophotometer (Unicam-UV 2) at wavelengths of 565 nm. The adsorbed amounts of Hg(II) ions were determined as follows:

$$q_e = \frac{V(C_0 - C_e)}{m_s} \quad (1)$$

C_0 (mg L⁻¹) is the initial Hg(II) concentration, C_e (mg L⁻¹) is the equilibrium Hg(II) concentration in aqueous solution, V (L) is the volume of the solution, m_s (g) is the *H. sericeum* amount, and q_e (mg g⁻¹) is the amount of calculated Hg(II) adsorption onto 1.0 g of *H. sericeum*.

RESULTS AND DISCUSSION

Characterization of Adsorbent

The FTIR spectrum of *H. sericeum* was evaluated in order to have an idea about the surface functional groups which are effective to the adsorption of Hg(II) ions. In the FTIR spectrum of *H. sericeum* (Figure 1), the important adsorption bands were observed at 3300 cm⁻¹ (due to bounded hydroxyl (–CHOH) or amine (–NH₂) groups), 2921 cm⁻¹ (due to –CH groups), 1617 cm⁻¹ (due to stretching vibration of carboxyl group (–C=O)), and 1024 cm⁻¹ (due to C–O stretching of alcohol and carboxylic acids) [26]. The SEM micrograph of *H. sericeum* gives an idea about the surface texture and morphology of the adsorbent. The *H. sericeum* has considerable numbers of homogenous and heterogeneous pores on its structure which are effective in Hg(II) ions adsorption (Figure 2).

Effect of Initial pH

The surface charge of an adsorbent, which is directly effective on the metal ion adsorption, highly depends on the initial solution pH. Hence the effect of pH on the Hg(II) ions adsorption was evaluated in the pH range of 2.0–8.0 by using 20 mg L⁻¹ of initial Hg(II) concentration and 2.0 g L⁻¹ of *H. sericeum* suspension. The adsorption amount of Hg(II) ions increased by the increase in the pH from 2.0 to 8.0 and reached to a maximum value (11.7 mg g⁻¹) at pH 6.0 (Figure 3). At lower pH values (pH < pH_{pzc}) the excessive H₃O⁺ ions occur in the aqueous solution hence the competition of H₃O⁺ ions with the positively charged Hg(II) ions for the active adsorption sites on the adsorbent surface and also the electrostatic repulsion between the positively charged adsorbent surface and Hg(II) ions induce the decrease in the adsorption amount [33,34]. Despite this, at higher pH values (pH > pH_{pzc}), the adsorption amount increased as a result of electrostatic interaction between the Hg(II) ions and the negatively charged adsorbent surface. Consequently, the optimum initial pH value was specified as 6.0 for the examination of further parameters. Similar results have been

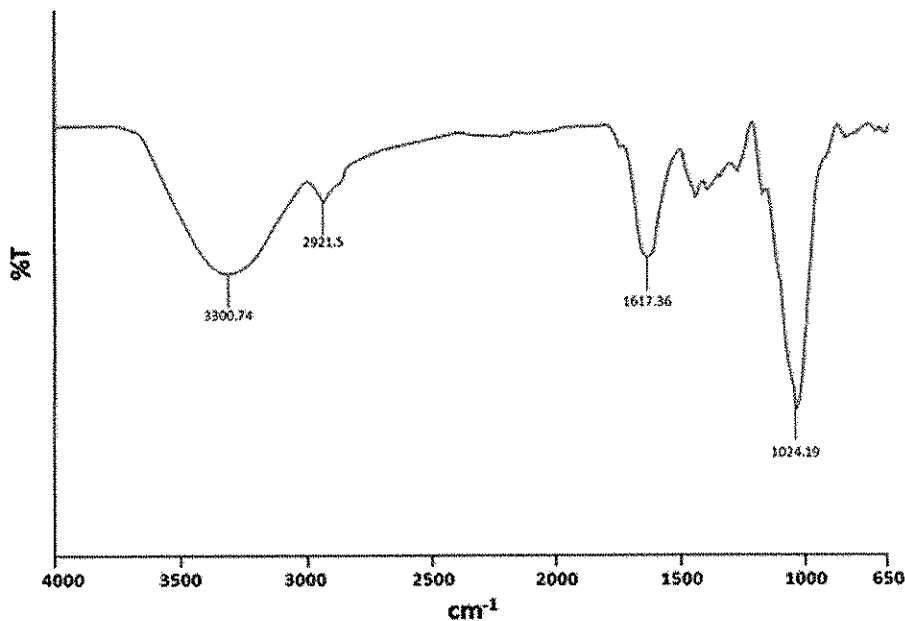


Figure 1. FTIR spectrum of *H. sericeum*. [Color figure can be viewed in the online issue, which is available at wileyonlinelibrary.com.]

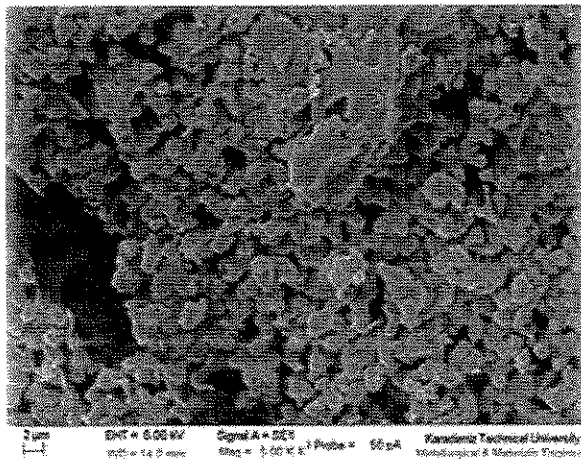


Figure 2. SEM image of *H. sericeum*.

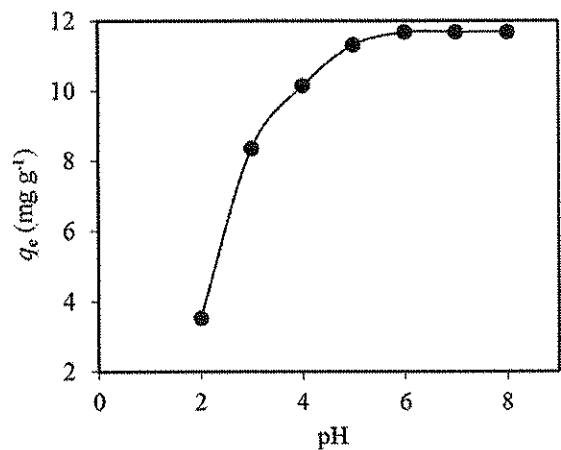


Figure 3. Effect of initial pH on Hg(II) adsorption onto *H. sericeum* (initial Hg(II) concentration: 20 mg L⁻¹; adsorbent concentration: 2.0 g L⁻¹).

reported by different researchers in the evaluation of Hg(II) ions biosorption onto modified *Phoenix dactylifera* biomass [21].

Effect of Contact Time and Evaluation of Adsorption Kinetics

In order to estimate the sufficient equilibrium time, the adsorption experiments were performed in the contact time range of 1–240 min by mixing 50 mg L⁻¹ of initial Hg(II) concentrations with 5.0 g L⁻¹ of *H. sericeum* at initial pH 6.0. The adsorption amount increased rapidly within the first 30 min of contact time due to the availability of a large number of vacant active sites on *H. sericeum* surface at the initial stage of the process [35]. Further increase in equilibrium time does not improve the adsorption capacity significantly, as a

result of saturation of the binding sites (Figure 4a). In order to make sure whether the adequate equilibrium time was obtained, the contact time was selected as 60 min for further experiments. Jafari and Cheraghi (2014) also reported the contact time as 60 min for the adsorption of Hg(II) ions by dried biomass of indigenous *Vibrio parahaemolyticus* PG02 [36].

The pseudo-first order, pseudo-second order, and intra-particle diffusion models were applied to the experimental data in order to determine the rate constants and to assess the dominant controlling mechanisms of the adsorption process.

The linear forms of the pseudo-first order [37] and pseudo-second order [38] models are given in Eqs. (2) and (3), respectively.

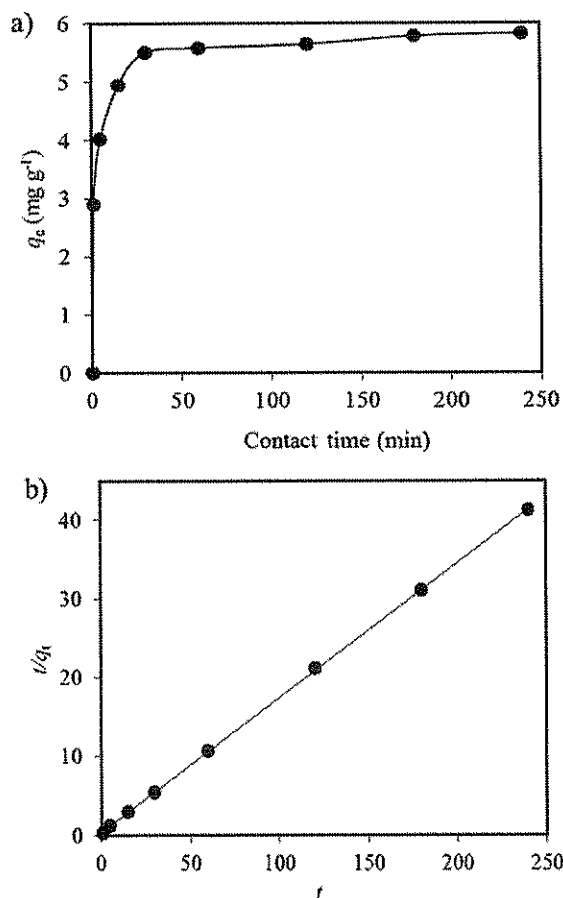


Figure 4. (a) Effect of contact time on Hg(II) uptake by *H. sericeum* (initial Hg(II) concentration: 50 mg L⁻¹; adsorbent concentration: 5.0 g L⁻¹; initial pH: 6.0), (b) pseudo-second order kinetic model.

$$\ln(q_e - q_t) = \ln q_e - k_1 t \quad (2)$$

$$\frac{t}{q_t} = \frac{1}{k_2 q_e^2} + \frac{t}{q_e} \quad (3)$$

where q_e (mg g⁻¹) and q_t (mg g⁻¹) are the amounts of the Hg(II) ions adsorbed on the *H. sericeum* at equilibrium and at any time t , respectively; and k_1 (min⁻¹) and k_2 (g mg⁻¹ min⁻¹) are the rate constants of the first order and second order models, respectively. The pseudo-first order constants (k_1 and $q_{e \text{ cal}}$) were calculated from the slope and intercept of the linear plot of $\ln(q_e - q_t)$ versus t , respectively while pseudo-second order constants (k_2 and $q_{e \text{ cal}}$) were determined from the intercept and slope of the plot of t/q_t

versus t (Figure 4b), respectively. All these parameters are presented in Table 2 with the related correlation coefficient (R^2) values. Contrary to the pseudo-first order model, the R^2 value obtained for the pseudo-second order model is relatively high and close to unity (>0.99), and also the calculated q_e value (5.85 mg g⁻¹) is compatible with the experimental value (5.82 mg g⁻¹), indicating that the adsorption of Hg(II) ions onto *H. sericeum* obeys the pseudo-second order model rather than pseudo-first order.

The rate controlling step of the process was evaluated by using the intraparticle diffusion model which is expressed as [39]:

$$q_t = k_{id} t^{1/2} + c \quad (4)$$

where k_{id} (mg g⁻¹ min^{-1/2}) is the intraparticle diffusion rate constant. The plot of q_t versus $t^{1/2}$ for Hg(II) adsorption onto *H. sericeum* indicates the existence of two kinetic steps in the process. The first and second steps are related to the diffusion of Hg(II) ions through the solution to the external surface of *H. sericeum* and the intraparticle diffusion of Hg(II) ions into the pores of *H. sericeum*, respectively. The intraparticle rate constants for the first step ($k_{id,1}$) and second step ($k_{id,2}$) were determined by using the plot of q_t versus $t^{1/2}$ and given in Table 2. The calculated $k_{id,2}$ value was lower than $k_{id,1}$, suggesting that the rate limiting step for Hg(II) adsorption is intraparticle diffusion. However, the plot did not pass through the origin so the intraparticle diffusion is not the only rate-limiting mechanism. Hence it can be concluded that in the adsorption process of Hg(II) ions onto *H. sericeum*, both intraparticle diffusion and surface sorption are effective on the rate-limiting step [40].

Effect of Initial Hg(II) Concentration and Adsorption Isotherms

In order to evaluate the effects of initial Hg(II) concentration on its uptake, the experiments were carried out with different initial Hg(II) concentrations in the range of 50–750 mg L⁻¹. Figure 5a shows the changes in both adsorption percentage (%) and adsorption amount (q_e , mg g⁻¹) with initial Hg(II) concentration. The adsorption amount increased from 5.7 to 72.0 mg g⁻¹ and the adsorption percentage decreased from 69.5 to 48.0% on increasing initial Hg(II) concentration from 50 to 750 mg L⁻¹. The higher initial Hg(II) concentration provided a significant driving force to overcome mass transfer resistance for Hg(II) transportation between the solution and the surface of *H. sericeum*, which increased the adsorption amount. On the other hand, the higher Hg(II) concentrations induced a saturation of the active adsorption sites on *H. sericeum* surface [21]. In other words, active adsorption sites were less available for Hg(II) binding at higher concentrations which decreased the adsorption percentage.

The adsorption isotherm data were fitted to Langmuir, Freundlich, and Dubinin Radushkevich isotherm models, in order to have an idea about the uptake mechanism of Hg(II) ions by *H. sericeum* and to reveal the mathematical relationship between the amount of Hg(II) adsorption per unit mass

Table 2. Parameters of the kinetic models for the adsorption of Hg(II) ions onto *H. sericeum*.

	Pseudo-first order kinetic model				Pseudo-second order kinetic model			Intraparticle diffusion model				
	$q_e \text{ exp}$ (mg g ⁻¹)	k_1 (min ⁻¹)	$q_e \text{ cal}$ (mg g ⁻¹)	R^2	k_2 (g mg ⁻¹ min ⁻¹)	$q_e \text{ cal}$ (mg g ⁻¹)	R^2	$k_{id,1}$ (mg g ⁻¹ min ^{-1/2})	R^2	$k_{id,2}$ (mg g ⁻¹ min ^{-1/2})	R^2	C
Hg(II)	5.82	-0.023	1.88	0.814	0.072	5.85	0.999	0.572	0.961	0.033	0.950	4.38

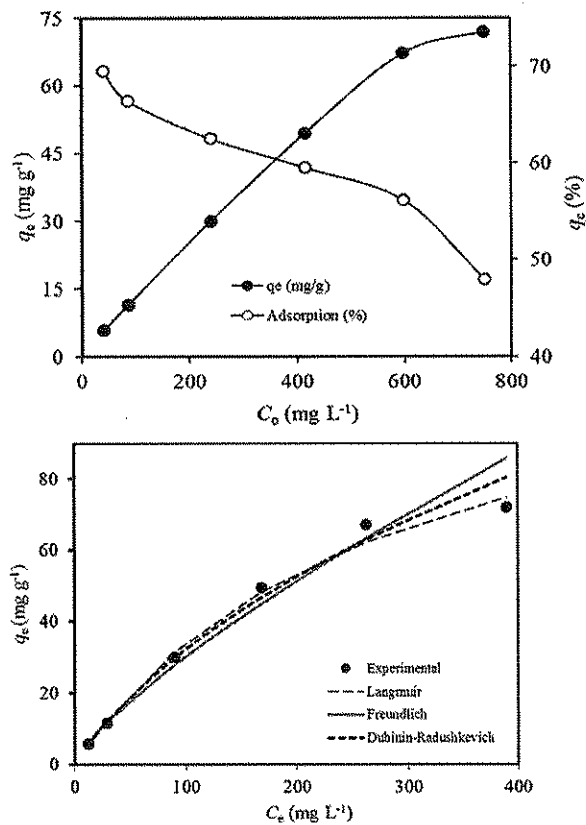


Figure 5. (a) Effect of initial Hg(II) concentration on its uptake by *H. sericeum* (initial pH:6.0; adsorbent concentration: 5.0 g L⁻¹; contact time: 60 min), (b) Comparison of equilibrium isotherms between the experimental and theoretical data for Hg(II) uptake.

of *H. sericeum* and the equilibrium concentration of Hg(II) ions in the solution.

According to Langmuir isotherm model [41], a monolayer adsorption takes place on homogenous adsorbent surface without any interaction between the adsorbed metal ions and all of the active binding sites on adsorbent surface have equal energy. On the other hand, the Freundlich isotherm model [42] describes the multilayer adsorption on heterogeneous adsorbent surface. The linear forms of Langmuir and Freundlich isotherm models are given in Eqs. (5) and (6), respectively.

$$\frac{C_c}{q_e} = \frac{C_c}{q_{max}} + \frac{1}{bq_{max}} \quad (5)$$

$$\ln q_e = \ln K_f + \frac{1}{n} \ln C_c \quad (6)$$

where q_e (mg g⁻¹) is the adsorbed amount of Hg(II) ions per unit mass of *H. sericeum* at equilibrium, C_c (mg L⁻¹) is the equilibrium concentration of Hg(II) ions in solution, q_{max} (mg g⁻¹) is the maximum adsorption capacity of *H. sericeum*, b (L mg⁻¹) is the energy of adsorption, K_f (mg g⁻¹) is the sorption capacity, and n is the sorption intensity. q_{max} and b values were calculated from the slope and intercept of the linear plot of C_c/q_e versus C_c , respectively by utilizing (5), while K_f and n values were determined from the intercept and slope of linear plot of $\ln q_e$ versus $\ln C_c$, respectively according to Eq. (6) (Table 3). The adsorption isotherm data of Hg(II) ions onto *H.*

Table 3. Isotherm constants for the adsorption of Hg(II) ions onto *H. sericeum*.

	Hg(II)
Langmuir isotherm model	
q_{max} (mg g ⁻¹)	128.2
b (L mg ⁻¹)	0.0036
R^2	0.973
Freundlich isotherm model	
K_f (mg g ⁻¹)	0.866
n	1.3
R^2	0.990
D-R isotherm model	
q_m (mg g ⁻¹)	533.26
β (kJ ² mol ⁻²)	0.0079
E (kJ mol ⁻¹)	7.96
R^2	0.996

sericeum were well-fitted to both Langmuir and Freundlich isotherm models (Figure 5b) since the obtained correlation coefficient (R^2) values are higher than 0.9, suggesting the availability of both homogeneous and heterogeneous active binding sites on the surface of *H. sericeum* [43]. The maximum monolayer adsorption capacity of *H. sericeum* was obtained as 128.2 mg g⁻¹ by using Langmuir equation. The feasibility of the presented adsorptive removal process was evaluated by using the separation factor (R_L) relative to Langmuir isotherm which is given in the following equation [44]:

$$R_L = \frac{1}{1 + b \cdot C_0} \quad (7)$$

where b (L mg⁻¹) is the Langmuir constant and C_0 (mg L⁻¹) is the initial Hg(II) concentration. For favorable adsorption, R_L values should be in the range of 0–1. In this study, the calculated R_L values ranged from 0.85 to 0.57 between 50 and 750 mg L⁻¹ of initial Hg(II) ion concentration, suggesting that the adsorption of Hg(II) ions onto *H. sericeum* is favorable under the studied conditions. In addition, the $1/n$ value obtained from the Freundlich isotherm model was smaller than unity, indicating that the Hg(II) ions were successfully separated from the aqueous solution [45].

The equilibrium data were also fitted to Dubinin Radushkevich (D-R) isotherm model in order to estimate whether the adsorption of Hg(II) ions onto *H. sericeum* is a physical or chemical process [46]. The linear form of the model can be expressed as:

$$\ln q_e = \ln q_m - \beta \epsilon^2 \quad (8)$$

where q_e (mol g⁻¹) is the amount of Hg(II) adsorbed per unit mass of *H. sericeum*, q_m (mol g⁻¹) is the monolayer adsorption capacity, β (mol² kJ⁻²) is the activity coefficient related to the mean sorption energy, ϵ is the Polanyi potential and can be calculated by the following equation:

$$\epsilon = RT \ln(1 + 1/C_c) \quad (9)$$

where R (8.314 J mol⁻¹ K⁻¹) is the universal gas constant, T (K) is the temperature, C_c (mol L⁻¹) is the equilibrium Hg(II) ion concentration in aqueous solution. The mean adsorption energy, E (kJ mol⁻¹), can be calculated using the following equation:

$$E = 1/(-2\beta)^{1/2} \quad (10)$$

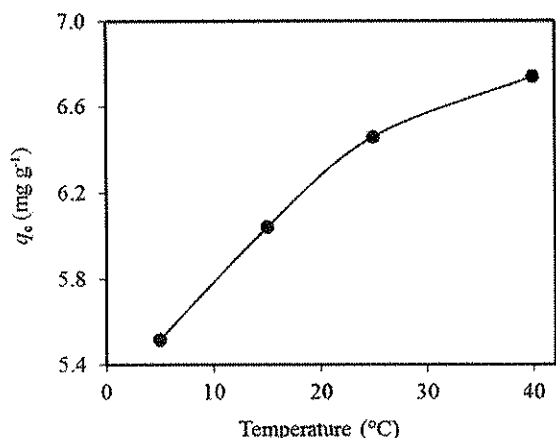


Figure 6. Effect of temperature on the adsorption of Hg(II) ions onto *H. sericeum* (initial Hg(II) concentration: 50 mg L⁻¹; adsorbent concentration: 5.0 g L⁻¹; initial pH: 6.0; contact time: 60 min).

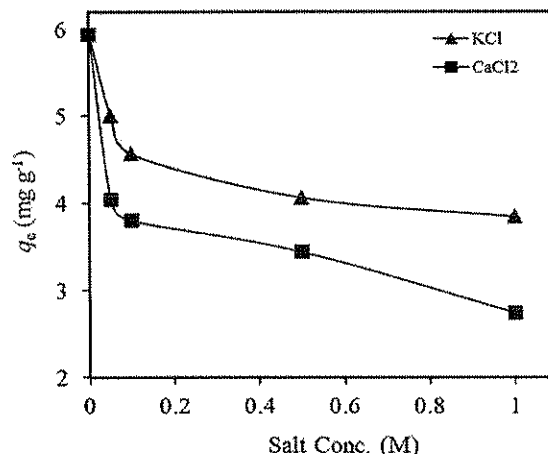


Figure 8. Effect of ionic strength on the adsorption of Hg(II) ions onto *H. sericeum* (initial Hg(II) concentration: 50 mg L⁻¹; adsorbent concentration: 5.0 g L⁻¹; initial pH: 6.0; contact time: 60 min).

Table 4. Thermodynamic parameters of Hg(II) adsorption onto *H. sericeum* at different temperatures.

T (°C)	Parameters		
	ΔG (kJ mol ⁻¹)	ΔS (J mol ⁻¹ K ⁻¹) ^a	ΔH (kJ mol ⁻¹) ^a
5	-1.70		
15	-2.40	63.29	15.83
25	-3.17		
40	-3.88		

^aMeasured between 278 and 313 K.

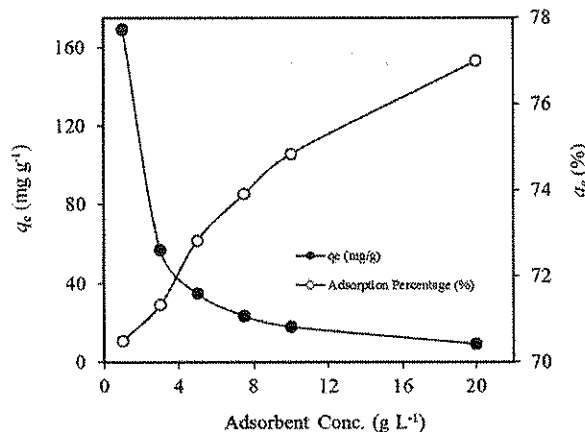


Figure 7. Effect of adsorbent concentration on Hg(II) uptake by *H. sericeum* (initial Hg(II) concentration: 250 mg L⁻¹; initial pH: 6.0; contact time: 60 min).

The slope of linear plot of $\ln q_e$ versus e^2 is equal to β , while the intercept gives q_m . The magnitude of E can be

used for estimating the adsorption type. There are three probabilities for E value: (i) for physical adsorption $E < 8$ kJ mol⁻¹, (ii) for ion exchange $8 < E < 16$ kJ mol⁻¹, and (iii) for chemical adsorption $E > 16$ kJ mol⁻¹ [47]. In the present study, the E value was calculated as 7.96 kJ mol⁻¹, suggesting that the mechanisms of the adsorption of Hg(II) ions onto *H. sericeum* is possibly a physical process.

Effect of Temperature and Thermodynamics of Adsorption

The effects of medium temperature on the removal efficiency of Hg(II) ions were investigated in the temperature range of 5–40°C. A slight increase in adsorption amount was obtained with an increase in temperature indicating the endothermic nature of the process (Figure 6). The reason may be ascribed to fact that the viscosity of the solution drops with the rise in temperature which leads to an increase in mobility and diffusion rate of Hg(II) ions, and thus more Hg(II) ions can interact with the active adsorption sites on *H. sericeum* surface [48].

Thermodynamic parameters including free energy change (ΔG), enthalpy (ΔH), and entropy (ΔS) have been determined using the following equations in order to investigate the thermodynamics behavior of the adsorption of Hg(II) ions onto *H. sericeum* [49].

$$\Delta G = -RT \ln K_d \quad (11)$$

$$K_d = q_e / C_e \quad (12)$$

$$\ln K_d = \frac{\Delta S}{R} - \frac{\Delta H}{RT} \quad (13)$$

where R is the universal gas constant (8.314 J mol⁻¹ K⁻¹), T is the temperature (K), K_d is the distribution coefficient, q_e (mg L⁻¹) and C_e (mg L⁻¹) are the equilibrium concentration of Hg(II) ions adsorbed onto *H. sericeum* and remained in the solution, respectively.

According to Eq. (13), the slope and intercept of the plot of $\ln K_d$ against $1/T$ is equal to $-\Delta H/R$ and $\Delta S/R$, respectively. The values of thermodynamic parameters for the adsorption of Hg(II) ions onto *H. sericeum* are given in Table 4. The spontaneity and feasibility of the present

Table 5. Comparison of Hg(II) adsorption onto different adsorbents.

Adsorbent	Adsorption capacity (mg g ⁻¹)	References
Sugarcane bagasse	35.71	[2]
Palm shell activated carbon impregnated with task-specific ionic-liquids	83.33	[3]
Unmodified bamboo leaf powder	27.11	[5]
Moss (<i>Drepanocladus revolvens</i>)	94.4	[27]
Romanian peat moss	98.94	[28]
Moss (<i>Funaria hygrometrica</i>)	52.0	[30]
Polyacrylonitrile-2-amino-1,3,4-thiadiazole chelating resin	526.9	[33]
<i>Vibrio parahaemolyticus</i> PG02	193.2	[36]
Xanthate functionalized magnetic graphene oxide	118.55	[52]
Aminated chitosan beads	89	[53]
Moss (<i>Homalothecium Sericeum</i>)	128.2	Present Study

adsorption process was proved by the negative ΔG values at different temperatures. On the other hand, the increase in the magnitude of ΔG values with the increase in temperature indicated that the process is more feasible at higher temperatures. The positive value of ΔS revealed the increased randomness at the solid/liquid interface during the adsorption of Hg(II) ions onto *H. sericeum* while the positive ΔH value indicated the endothermic nature of the process.

Effect of Adsorbent Concentration

In adsorptive removal processes, it is important to use suitable adsorbent amounts to provide the sufficient interactions between adsorbate and the active adsorption sites on the adsorbent surface [50]. Therefore, the effects of adsorbent amount on the uptake of Hg(II) ions were evaluated within the *H. sericeum* concentration range of 1.0–20.0 g L⁻¹. When the amount of *H. sericeum* was increased from 1.0 to 20.0 g L⁻¹, as a result of increase in the number of available adsorption sites, the removal percentage increased from 70 to 77%. On the other hand, the higher adsorbent amount leads to a decrease in total surface area by agglomeration and to formation of unsaturated adsorption sites, and thus the adsorption amount decreased from 169.2 to 9.2 mg g⁻¹ on increasing the amount of *H. sericeum* from 1.0 to 20.0 g L⁻¹ (Figure 7).

Effect of Ionic Strength

The effects of the presence of ionic strengths on the Hg(II) adsorption was evaluated by using KCl and CaCl₂ as model salts in the concentration range of 0.05–1.0 mol L⁻¹. The results indicated that the adsorption of Hg(II) ions by *H. sericeum* is inhibited considerably at high electrolyte concentrations, namely the removal efficiency of Hg(II) ions decreased from 5.8 to 3.8 and 2.7 mg g⁻¹ by increasing the concentration of KCl and CaCl₂ salts from 0 to 1.0 mol L⁻¹, respectively (Figure 8). The competition between the Hg(II) and salt's cations for the active adsorption sites on the adsorbent surface and also the blocking of these sites in the presence of high ionic strengths may cause these results. On the other hand, the further decrease when used CaCl₂ is an expected result since divalent cations may have more inhibition and competition effects than monovalent cations [21,51].

CONCLUSIONS

The adsorption potential of Hg(II) ions onto *H. sericeum* was evaluated in the present investigation. The process was highly pH-dependent and the maximum Hg(II) adsorption was observed at initial pH 6.0. The kinetics evaluation indicated that the equilibrium can be reached within 60 min of contact time and the process followed well the pseudo-second order model. The adsorption isotherms fitted well to both Langmuir and Freundlich isotherm models indicating the homogeneous and heterogeneous distribution of the active adsorption sites on the adsorbent surface. The adsorption amount of Hg(II) ions onto *H. sericeum* increased when increasing the temperature from 5 to 40°C and the thermodynamic parameters including ΔG , ΔH , and ΔS indicated the spontaneous and endothermic nature of the process. The maximum adsorption capacity of *H. sericeum* was found to be 128.2 mg g⁻¹ from Langmuir model equations. This value was compared with various adsorbents previously reported in the literature [2,3,5,27,28,30,33,36,52,53]. As can be seen from Table 5, the removal efficiency of *H. sericeum* (128.2 mg g⁻¹) was found to be better than other moss species, utilized for Hg(II) adsorption, which are Romanian peat moss (98.94 mg g⁻¹), *Funaria hygrometrica* (52.0 mg g⁻¹), and *Drepanocladus revolvens* (94.4 mg g⁻¹).

The results of the present study proved that *H. sericeum* can be used as a natural, readily available and effective adsorbent in removal of Hg(II) ions from aqueous solutions by batch adsorption techniques.

ACKNOWLEDGMENTS

The authors are grateful for the financial support of both the Unit of the Scientific Research Projects of Gumushane University and Karadeniz Technical University. The authors also would like to thank Dr. Turan Özdemir for identification of the moss samples.

LITERATURE CITED

- Niu, Y., Qu, R., Liu, X., Mu, L., Bu, B., Sun, Y., Chen, H., Meng, Y., Meng, L., & Cheng, L. (2014). Thiol-functionalized polysilsesquioxane as efficient adsorbent for adsorption of hg(II) and mn(II) from aqueous solution, *Materials Research Bulletin*, 52, 134–142.
- Khoramzadeh, E., Nasernejad, B., & Halladj, R. (2013). Mercury biosorption from aqueous solutions by sugarcane bagasse, *Journal of the Taiwan Institute of Chemical Engineers*, 44, 266–269.
- Ismail, A.A., Aroua, M.K., & Yusoff, R. (2013). Palm shell activated carbon impregnated with task-specific ionic-liquids as a novel adsorbent for the removal of mercury from contaminated water, *The Chemical Engineering Journal*, 225, 306–314.
- Raji, F. & Pakizeh, M. (2014). Kinetic and thermodynamic studies of Hg(II) adsorption onto MCM-41 modified by ZnCl₂, *Applied Surface Science*, 301, 568–575.
- Mondal, D.K., Nandi, B.K., & Purkait, M.K. (2013). Removal of mercury (II) from aqueous solution using bamboo leaf powder: Equilibrium, thermodynamic and kinetic studies, *The Journal of Environmental Chemical Engineering*, 1, 891–898.
- Boening, D.W. (2000). Ecological effects, transport, and fate of mercury: A general review, *Chemosphere*, 40, 1335–1351.
- World Health Organisation (2011). Guidelines for drinking-water quality (4th Edition). World Health Organisation, Geneva, Switzerland.
- Chauhan, D. & Sankaramakrishnan, N. (2008). Highly enhanced adsorption for decontamination of lead ions from battery wastewaters using chitosan functionalized with xanthate, *Bioresource Technology*, 99, 9021–9024.

9. Pal, P. & Banat, F. (2014). Comparison of heavy metal ions removal from industrial lean amine solvent using ion exchange resins and sand coated with chitosan, *Journal of Natural Gas Science and Engineering*, 18, 227–236.
10. Matlock, M.M., Howerton, B.S., & Atwood, D.A. (2002). Chemical precipitation of heavy metals from acid mine drainage, *Water Research*, 36, 4757–4764.
11. Bessbousse, H., Rhlalou, T., Verchère, J.F., & Lebrun, L. (2008). Sorption and filtration of hg(II) ions from aqueous solutions with a membrane containing poly(ethyleneimine) as a complexing polymer, *Journal of Membrane Science*, 325, 997–1006.
12. Mohsen-Nia, M., Montazeri, P., & Modarress, H. (2007). Removal of Cu²⁺ and Ni²⁺ from wastewater with a chelating agent and reverse osmosis processes, *Desalination*, 217, 276–281.
13. Senthil Kumar, P., Senthamarai, C., & Durgadevi, A. (2014). Adsorption kinetics, mechanism, isotherm, and thermodynamic analysis of copper ions onto the surface modified agricultural waste, *Environmental Progress & Sustainable Energy*, 33, 28–37.
14. Fu, F. & Wang, Q. (2011). Removal of heavy metal ions from wastewaters: A review, *The Journal of Environmental Management*, 92, 407–418.
15. Murugesan, M.A., Vidhyadevi, T., Kalaivani, S.S., Baskaralingam, P., Anuradha, C.D., & Sivanesan, S. (2014). Kinetic studies and isotherm modeling for the removal of Ni²⁺ and Pb²⁺ ions by modified activated carbon using sulfuric acid, *Environmental Progress & Sustainable Energy*, 33, 844–854.
16. Naiya, T.K., Bhattacharya, A.K., & Das, S.K. (2008). Adsorption of Pb(II) by sawdust and neem bark from aqueous solutions, *Environmental Progress & Sustainable Energy*, 27, 313–328.
17. Vankar, P.S., Sarswat, R., & Sahu, R. (2012). Biosorption of zinc ions from aqueous solutions onto natural dye waste of *Hibiscus rosa sinensis*: Thermodynamic and kinetic studies, *Environmental Progress & Sustainable Energy*, 31, 89–99.
18. González, P.G. & Pliego-Cuervo, Y.B. (2014). Adsorption of cd(II), hg(II) and zn(II) from aqueous solution using mesoporous activated carbon produced from *Bambusa vulgaris striata*, *Chemical Engineering Research and Design*, 92, 2715–2724.
19. Wang, X., Sun, R., & Wang, C. (2014). pH dependence and thermodynamics of Hg(II) adsorption onto chitosan-poly(vinyl alcohol) hydrogel adsorbent, *Colloids and Surfaces A: Physicochemical and Engineering Aspects*, 441, 51–58.
20. Allouchea, F.N., Guibal, E., & Mameri, N. (2014). Preparation of a new chitosan-based material and its application for mercury sorption, *Colloids and Surfaces A: Physicochemical and Engineering Aspects*, 446, 224–232.
21. Rajamohan, N., Rajasimman, M., & Dilipkumar, M. (2014). Parametric and kinetic studies on biosorption of mercury using modified *Phoenix dactylifera* biomass, *Journal of the Taiwan Institute of Chemical Engineers*, 45, 2622–2627.
22. Arshadi, M. (2015). Manganese chloride nanoparticles: A practical adsorbent for the sequestration of Hg(II) ions from aqueous solution, *Chemical Engineering Journal*, 259, 170–182.
23. Sari, A., Mendil, D., Tuzen, M., & Soylak, M. (2009). Biosorption of palladium(II) from aqueous solution by moss (*Racomitrium lanuginosum*) biomass: Equilibrium, kinetic and thermodynamic studies, *Journal of Hazardous Materials*, 162, 874–879.
24. Koz, B. & Cevik, U. (2014). Lead adsorption capacity of some moss species used for heavy metal analysis, *Ecological Indicators*, 36, 491–494.
25. Sharma, S. (2009). Study on impact of heavy metal accumulation in *Brachybotryum populeum* (Hedw.) B.S.G., *Ecological Indicators*, 9, 807–811.
26. Sari, A., Mendil, D., Tuzen, M., & Soylak, M. (2008). Biosorption of Cd(II) and Cr(III) from aqueous solution by moss (*Hylocomium splendens*) biomass: Equilibrium, kinetic and thermodynamic studies, *Chemical Engineering Journal*, 144, 1–9.
27. Sari, A. & Tuzen, M. (2009). Removal of mercury(II) from aqueous solution using moss (*Drepanocladus revolvens*) biomass: Equilibrium, thermodynamic and kinetic studies, *Journal of Hazardous Materials*, 171, 500–507.
28. Bulgariu, L., Ratoi, M., Bulgariu, D., & Macoveanu, M. (2009). Adsorption potential of mercury(II) from aqueous solutions onto Romanian peat moss, *Journal of Environmental Science and Health, Part A*, 44, 700–706.
29. Kondoh, M., Fukuda, M., Azuma, M., Ooshima, H., & Kato, J. (1998). Removal of mercury ion by the moss *Pohlia flexuosa*, *Journal of Fermentation and Bioengineering*, 86, 197–201.
30. Krishna, M.V.B., Karunasagar, D., & Arunachalam, J. (2004). Sorption characteristics of inorganic, methyl and elemental mercury on lichens and mosses: Implication in biogeochemical cycling of mercury, *The Journal of Atmospheric Chemistry*, 49, 317–328.
31. APHA. (1985). Standard methods for the examination of water and wastewater (18th Edition), Washington, DC: American Public Health Association.
32. Boehm, H.P. (2002). Surface oxides on carbon and their analysis: A critical assessment, *Carbon*, 40, 145–149.
33. Xiong, C., Li, Y., Wang, G., Fang, L., Zhou, S., Yao, C., Chen, Q., Zheng, X., Qi, D., Fu, Y., & Zhu, Y. (2015). Selective removal of Hg(II) with polyacrylonitrile-2-amino-1,3,4-thiadiazole chelating resin: Batch and column study, *The Chemical Engineering Journal*, 259, 257–265.
34. Li, R., Liu, L., & Yang, F. (2013). Preparation of polyaniline/reduced graphene oxide nanocomposite and its application in adsorption of aqueous Hg(II), *The Chemical Engineering Journal*, 229, 460–468.
35. Joo, J.H., Hassan, S.H.A., & Oh, S.E. (2010). Comparative study of biosorption of Zn²⁺ by *Pseudomonas aeruginosa* and *Bacillus cereus*, *International Biodeterioration and Biodegradation*, 64, 734–741.
36. Jafari, S.A. & Cheraghi, S. (2014). Mercury removal from aqueous solution by dried biomass of indigenous *Vibrio parahaemolyticus* PG02: Kinetic, equilibrium, and thermodynamic studies, *International Biodeterioration and Biodegradation*, 92, 12–19.
37. Lagergren, S. (1898). About the theory of so-called adsorption of soluble substance, *Kungliga Svenska Vetenskapsakademiens Handlingar*, 24, 1–39.
38. Ho, Y.S. & McKay, G. (1998). Kinetic models for the sorption of dye from aqueous solution by wood, *Journal of Environmental Science and Health, Part B: Process Safety and Environmental Protection*, 76, 183–191.
39. Weber, W.J., Jr. & Morriss, J.C. (1963). Kinetics of adsorption on carbon from solution, *Journal of the Sanitary Engineering Division American Society of Civil Engineers*, 89, 31–60.
40. Fu, J., Chen, Z., Wang, M., Liu, S., Zhang, J., Zhang, J., Han, R., & Xu, Q. (2015). Adsorption of methylene blue by a high-efficiency adsorbent (polydopamine microspheres): Kinetics, isotherm, thermodynamics and mechanism analysis, *The Chemical Engineering Journal*, 259, 53–61.
41. Langmuir, I. (1918). The adsorption of gases on plane surfaces of glass, mica and platinum, *Journal of the American Chemical Society*, 40, 1361–1403.

42. Freundlich, H.M.F. (1906). Über die adsorption in lösungen, *Zeitschrift für Physikalische Chemie*, 57, 385–470.
43. Zeng, S., Duan, S., Tang, R., Li, L., Liu, C., & Sun, D. (2014). Magnetically separable $\text{Ni}_0.6\text{Fe}_{2.4}\text{O}_4$ nanoparticles as an effective adsorbent for dye removal: Synthesis and study on the kinetic and thermodynamic behaviors for dye adsorption, *The Chemical Engineering Journal*, 258, 218–228.
44. Hall, K.R., Eagleton, L.C., Acrivos, A., & Vermeulen, T. (1966). Pore- and solid-diffusion kinetics in fixed-bed adsorption under constant-pattern conditions, *Industrial & Engineering Chemistry Fundamentals*, 5, 212–223.
45. Kamari, A., Yusoff, S.N.M., Abdullah, F., & Putra, W.P. (2014). Biosorptive removal of Cu(II), Ni(II) and Pb(II) ions from aqueous solutions using coconut dregs residue: Adsorption and characterization studies, *The Journal of Environmental Chemical Engineering*, 2, 1912–1919.
46. Dubinin, M.M. & Radushkevich, L.V. (1947). Equation of the characteristics curve of activated charcoal, *Chemisches Zentralblatt*, 1, 875
47. Lin, S.H. & Juang, R.S. (2002). Heavy metal removal from water by sorption using surfactant-modified montmorillonite, *The Journal of Hazardous Materials*, 92, 315–326.
48. Saadat, S., Karimi-Jashni, A., & Doroodmand, M.M. (2014). Synthesis and characterization of novel single-walled carbon nanotubes-doped walnut shell composite and its adsorption performance for lead in aqueous solutions, *The Journal of Environmental Chemical Engineering*, 2, 2059–2067.
49. Smith, J.M., & Van Ness, H.C. (1987). *Introduction to chemical engineering thermodynamics* (4th Edition), Singapore: McGraw-Hill.
50. Ren, Y., Abbood, H.A., He, F., Peng, H., & Huang, K. (2013). Magnetic EDTA-modified chitosan/ $\text{SiO}_2/\text{Fe}_3\text{O}_4$ adsorbent: Preparation, characterization, and application in heavy metal adsorption, *Chemical Engineering Journal*, 226, 300–311.
51. Tso, C.P., Zhung, C.M., Shih, Y.H., Tseng, Y.M., Wu, S.C., & Doong, R.A. (2010). Stability of metal oxide nanoparticles in aqueous solutions, *Water Science and Technology*, 61, 127–133.
52. Cui, L., Guo, X., Wei, Q., Wang, Y., Gao, L., Yan, L., Yan, T., & Du, B. (2015). Removal of mercury and methylene blue from aqueous solution by xanthate functionalized magnetic graphene oxide: Sorption kinetic and uptake mechanism. *Journal of Colloid and Interface Science*, 439, 112–120.
53. Wang, L., Xing, R., Liu, S., Cai, S., Yu, H., Feng, J., Li, R., & Li, P. (2010). Synthesis and evaluation of a thiourea-modified chitosan derivative applied for adsorption of Hg(II) from synthetic wastewater, *International Journal of Biological Macromolecules*, 46, 524–528.